

Simulated equilibrium and nonequilibrium interfaces in a lattice model

Z. Jiang and C. Ebner

Department of Physics, Ohio State University, Columbus, Ohio 43210

(Received 29 February 1988)

We have studied the properties of equilibrium and nonequilibrium $(d-1)$ -dimensional interfaces via Monte Carlo simulations of a d -dimensional solid-on-solid model with $d=2$ and 3. At equilibrium, we examine the intrinsic width of the interface and the interfacial profile as functions of both the lateral size L of the system and the applied gravitational field g ; we have studied also the height-height correlation function as a function of both separation and g in two dimensions. Our results are consistent with theories of these properties relying on exact (in an appropriate limit) solution of the model for the case of $d=2$ and on capillary-wave theory for $d=3$. The nonequilibrium interfaces studied are those which arise between a growing wetting film and a bulk phase. We look at the intrinsic width of the interface and at the interfacial profile in the large- L limit as functions of time and of the interaction between the substrate and adsorbate. For $d-1$ equal to both 1 and 2, and for all adsorbate-substrate potentials used, the width grows at a rate which is independent of this potential; the rate is consistent with fluctuation-dominated growth mechanisms. The profiles have the same shape as the equilibrium profiles. In particular we find for $d-1=1$ that the width varies with time as $w \sim t^{1/4}$, which is the same as the rate of growth of the film thickness in the fluctuation regime.

I. INTRODUCTION

In a previous paper,¹ hereafter referred to as I, we presented the results of Monte Carlo (MC) simulations of the growth of wetting films on a substrate as modeled by a d -dimensional solid-on-solid (SOS) model. Emphasis in that work was placed on the rate of growth of the films as functions of time in the limit that the lateral size L of the system is large enough to play no role. The results were compared with the predictions of Lipowsky,² based on analysis of an effective interface model, and were found to be in agreement. This paper is devoted to further MC study of the SOS model with emphasis on the properties of the interface between the growing film and the bulk phase and also on the properties of an equilibrium interface between two coexisting bulk phases. In the latter case we look, in particular, on the interfacial properties as functions of L and of the gravitational field g acting on the system, and we are able to compare our results with analytic calculations using this and other models.³⁻¹¹ In particular, for the one-dimensional interface, there are exact calculations, in the continuum limit, of some properties of the equilibrium interface in the SOS model.³⁻⁶ Similar calculations exist for the Gaussian column model⁷ and for the Ising model.^{8,9} We have extended the calculations of van Leeuwen and Hilhorst,³ in particular, to include a prediction of the height-height correlation function and have carried the calculation of this function and the profile shape through to obtain simple results at small g . For the two-dimensional equilibrium interface, there are approximate analytic theories, e.g., the capillary-wave model,^{10,11} which allow for the determination of properties such as the width, the profile, and various correlation functions. Wherever feasible, we have compared our simulations with the appropriate analytic predictions.

In the case of nonequilibrium interfaces, there are general predictions of the behavior of the liquid-gas interfacial width in the fluctuation-dominated regime;¹² also, Schmidt and Binder have studied the problem of the interface between a growing film and bulk phase within the context of a time-dependent Landau-Ginzburg model.¹³

Section II of this paper contains a description of our model and Monte Carlo methods, and Sec. III presents the results. A summary is contained in Sec. IV. The Appendix presents a summary of the exact solution³ of the model for an equilibrium one-dimensional interface.

II. MODEL AND METHODS

As in I, we use a solid-on-solid model with nearest-neighbor ferromagnetic interactions $J/2$ on a $(d-1)$ -dimensional square lattice parallel to the surface of the substrate, or, more generally, perpendicular to the z axis; $d=2$ or 3. At any site i of the lattice there is a column of adsorbate atoms of height h_i . In the case of adsorption, $h_i=0, 1, 2, \dots$, and for the case of an interface between two bulk phases, h_i can take on any integral value. The Hamiltonian is

$$\mathcal{H} - \mu N = (J/2) \sum_{\langle i, j \rangle} |h_i - h_j| + \sum_i U(h_i), \quad (1)$$

where

$$U(h_i) = V(h_i) - \mu h_i \quad (2)$$

in the case of the adsorption problem, and

$$U(h_i) = gh_i^2 \quad (3)$$

for the interface between bulk phases. In these equations, μ is the chemical potential, $V(h_i)$ is the adsorbate-

substrate interaction, and g is the gravitational field; $\langle i, j \rangle$ denotes a sum over all nearest-neighbor pairs of columns. Bulk two-phase coexistence obtains for $\mu=0$. The substrate potentials used are either

$$V(h) \equiv 0 \quad (4)$$

or

$$V(h) = \begin{cases} 7.85J & \text{if } h=0, \\ 4.2J/h^p & \text{if } h>0. \end{cases} \quad (5)$$

In the simulations of film growth reported here, we have used primarily $p=1$ and 2. In two dimensions (interface dimension of 1), the temperature used was $T=0.5J/k$, and in three dimensions, $T=0.8J/k$ which is well above the roughening temperature¹⁴ $T_R \approx 0.6J/k$; k is Boltzmann's constant. The system size L used ranged from 50 to 1000 in $d=2$ and from 5 to 200 in $d=3$.

Quantities calculated include the height-height correlation function at separation k , $H(k)$; the intrinsic width of the interface w ; the intrinsic profile $n(z)$, and the coverage Γ . These quantities may be defined by the following formulas:

$$\Gamma(t) = L^{1-d} \sum_i h_i(t), \quad (6)$$

$$w(t) = \left[L^{1-d} \sum_i [h_i(t) - \Gamma(t)]^2 \right]^{1/2}, \quad (7)$$

$$H(k, t) = L^{1-d} \sum_i [h_{i+k}(t) - \Gamma(t)][h_i(t) - \Gamma(t)], \quad (8)$$

and

$$n(z, t) = L^{1-d} \sum_i \Theta[h_i(t) - \Gamma(t) - z]. \quad (9)$$

where Θ is a step function.

In the case of nonequilibrium profiles, each of these quantities is a function of time and is determined from the simulations by averaging over many runs starting each run from an initial configuration with all h_i set equal to zero. Typically, some 50 MC runs of 10^5 MCS (Monte Carlo steps per site) were utilized. For equilibrium profiles, w , H , and n are independent of time and may be determined from a single sufficiently long MC run.

III. RESULTS

A. Equilibrium interfaces

We shall discuss in turn our results for $d=2$ and 3. In two dimensions we consider first the case of $g=0$ which is special in that the intrinsic width of the interface diverges with the size L of the system. We have done a series of simulations for $w(L)$ using values of L ranging from 50 to 525 and $T=0.5J/k$. The results are shown in Fig. 1 which is a log-log plot of w versus L . The solid line is the result of a least-squares fit to the data (slope equals 0.506 ± 0.057). From, e.g., capillary-wave theory^{10,11} or exact treatment of the Gaussian column model,⁷ one expects $w \sim L^{1/2}$.

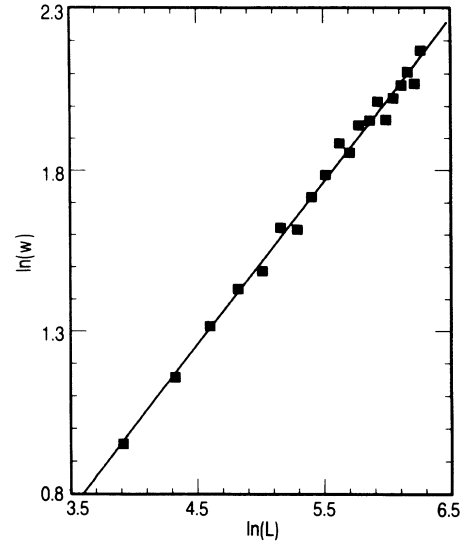


FIG. 1. The logarithm of w is plotted against that of L with $g=0$ and $T=0.5J/k$ for equilibrium interfaces in $d=2$; the solid line is from a least-squares fit to the simulation results (slope of 0.506 ± 0.057).

Figure 2 shows, for $L=400$, simulated profile $n(z)$ versus z and also the analytic function

$$f(z) = [1 - \text{erf}(z/\sqrt{2}w)]/2; \quad (10)$$

$\text{erf}(x)$ is the error function, see Eq. (A19). Equation (10) is the expected form of the profile on the basis of analytic calculations⁷ or capillary-wave theory.¹⁰ For w we have used the value inferred from the simulations, i.e., 7.2. Agreement of the simulated profile with the predicted

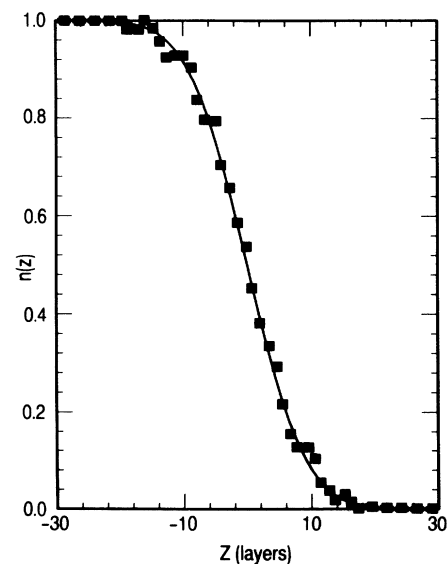


FIG. 2. The density $n(z)$ of an equilibrium interfacial profile is shown as a function of z for $2g/J=0$, $L=400$, $T=0.5J/k$, and $d=2$. The solid line is the theoretical prediction, Eq. (10), using $w=7.2$ as inferred from the simulations.

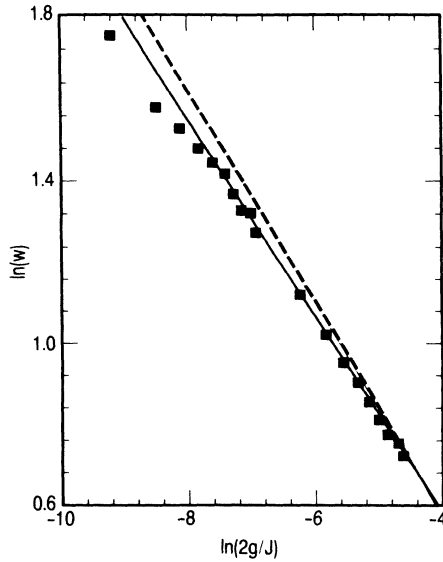


FIG. 3. The logarithm of w is plotted against that of $2g/J$ for equilibrium profiles with $L=400$ and $T=0.5J/k$ in $d=2$. The solid line is a least-squares fit (slope of -0.24 ± 0.02) to the ten largest- g points; the dashed line is the prediction from the exact solution of the SOS model in the continuum limit and for $L \rightarrow \infty$.

one is seen to be quite good. Equally good agreement was obtained for other values of L .

We turn now to the g dependence of the equilibrium width and profile for $d=2$. We have done simulations for several values of g and for $L=400$ which is large enough that the results are size independent at the larger values of g . The interface width is predicted³ (see Appendix) to vary as $g^{-1/4}$. Figure 3 shows a log-log plot of w

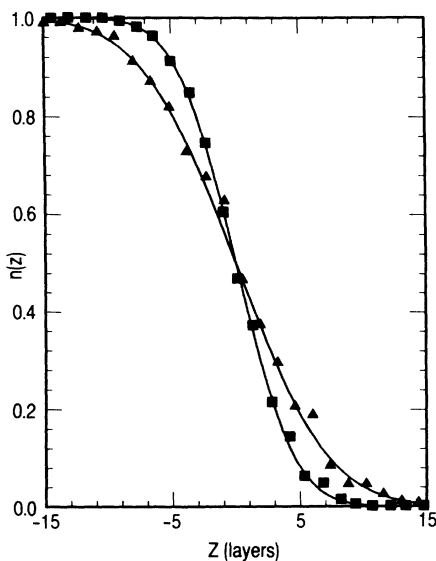


FIG. 4. The densities $n(z)$ of equilibrium profiles for $2g/J=0.001$ (■) and $g=0.0001$ (▲) are shown as functions of z for $L=400$, $T=0.5J/k$, and $d=2$. The solid lines are the theoretical prediction, Eq. (10), using w as inferred from the simulations.

versus $2g/J$ at $T=0.5J/k$. The solid line (slope of -0.24 ± 0.02) is the result of a least-squares fit to the data for the ten largest values of g . One can see in the simulation results a tendency toward saturation of w at the smallest values of g . The $g=0$ width of the interface at these values of L and T is 7.2, cf. Figs. 1 and 2, and so w will tend toward this value as $g \rightarrow 0$. The dashed line in the figure is the predicted value of $w(g)$ for $L \rightarrow \infty$, small g , and in the continuum limit, taken from Eq. (29); the agreement is less than perfect, most probably as a consequence of size effects and perhaps also as a consequence of the difference between the discrete model and the continuum limit. Figure 4 shows the profiles at $T=0.5J/k$ and $L=400$ for $2g/J=0.001$ and $2g/J=0.0001$; the solid lines are given by Eq. (10) with widths w equal to 3.60 and 5.75, respectively; these are the values which may be inferred from the simulations, Fig. 3. Once again, agreement of simulated and analytic results is good.

Figure 5 is a plot of $\ln[H(k)/H(0)]$ versus k for $L=800$, $T=0.5J/k$, and $2g/J=0.0001$, 0.0005, and 0.001 in two dimensions; analytic calculations of $H(k)$ presented in the Appendix demonstrate that for sufficiently small g it should fall off exponentially with distance with an exponent proportional to $k\sqrt{g}$. The inset in Fig. 5 plots $\ln[H(k)/H(0)]/\beta gh_0^2$ (see the Appendix for a definition of h_0), where $\beta=1/kT$, for the same three values of g , all data lie very nearly on a straight

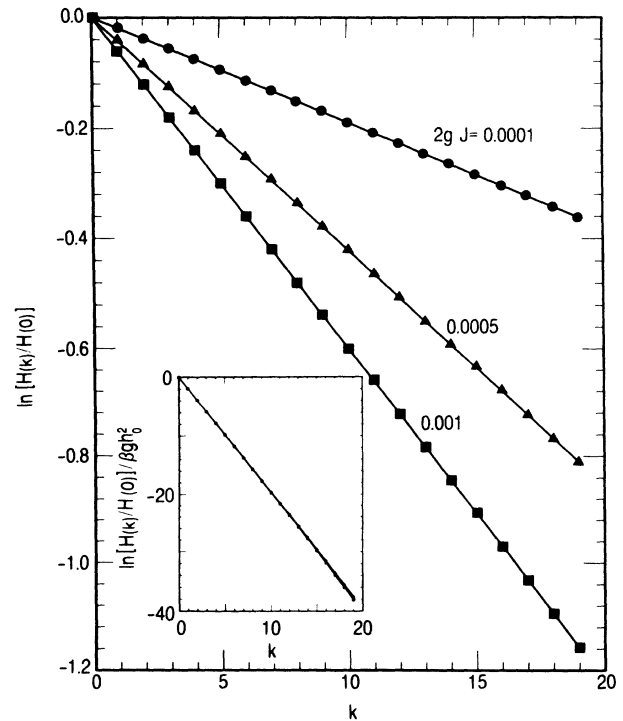


FIG. 5. The logarithm of the height-height correlation function scaled by $H(0)$, is plotted against the separation k for $2g/J=0.0001$ (●), $2g/J=0.0005$ (▲), and $2g/J=0.001$ (■), for $L=800$, $T=0.5J/k$, and $d=2$. The inset shows the same, but the quantity plotted along the ordinate is further scaled by βgh_0^2 to obtain a g -independent quantity as predicted by the analytic solution; see the Appendix.

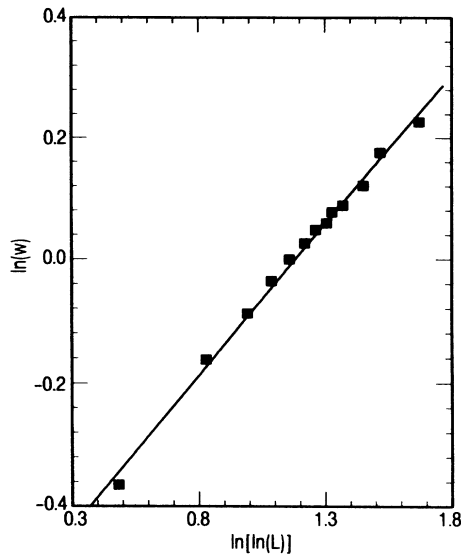


FIG. 6. For $d=3$, we plot $\ln w$ vs $\ln(\ln L)$ at $g=0$ and $T=0.8J/k$ for $5 \leq L \leq 200$. The line is a least-squares fit to the simulation results; it has a slope of 0.493 ± 0.008 .

line, demonstrating the expected g dependence.

For the equilibrium two-dimensional ($d=3$) interface, one has approximate models, such as the capillary-wave model,^{10,11} with which to compare the simulation results. The predicted variation of w with L for $g=0$ is $w \sim \sqrt{\ln L}$. At $T=0.8J/k$ we plot in Fig. 6 $\ln w$ versus $\ln(\ln L)$ for values of L from 5 to 200; the solid line is a least-squares fit to the data (slope equals 0.493 ± 0.008). The results of the simulations may be said to be in good agreement with the theoretical prediction. Note, however, that the interface width is only of order 1. Figure 7 shows the profile $n(z)$ versus z for $L=50$, and

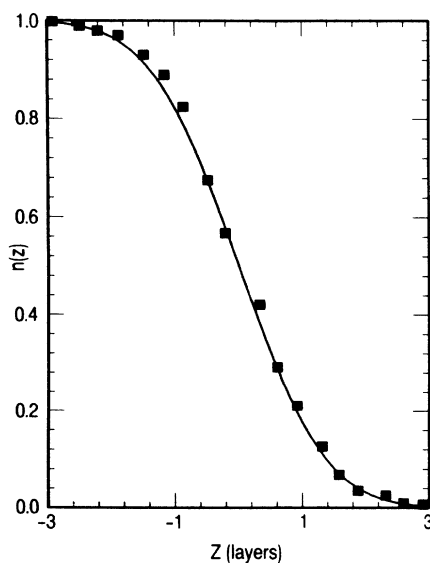


FIG. 7. For $d=3$, we plot $n(z)$ vs z for $g=0$, $L=50$, and $T=0.8J/k$. The solid line is the error function profile with $w=1.08$ as inferred from the simulations.

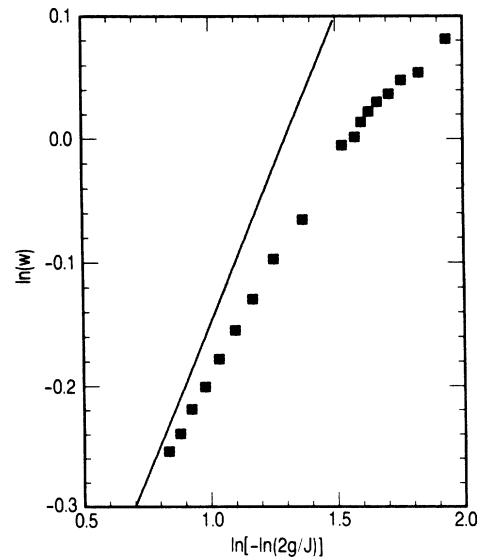


FIG. 8. For $d=3$ we plot $\ln w$ vs $\ln[-\ln(2g/J)]$ at $T=0.8J/k$ and $L=50$. The data fit a straight line of slope ≈ 0.4 at the larger values of g ; the theoretical prediction of the slope in the large- L limit is $\frac{1}{2}$, shown by the solid line.

$T=0.8J/k$; the solid line is the error function profile, Eq. (10), with $w=1.08$, the value given by the simulations.

We have also done simulations of the $d=3$ interface for $g \neq 0$. Because of the very small width of the $g=0$ interface at the largest value of L that we are able to treat, the results are not satisfactorily conclusive regarding the expected¹¹ $w \sim \sqrt{-\ln g}$ behavior. Figure 8 shows a plot of $\ln w$ versus $\ln[-\ln(2g/J)]$ for $T=0.8J/k$ and $L=50$.

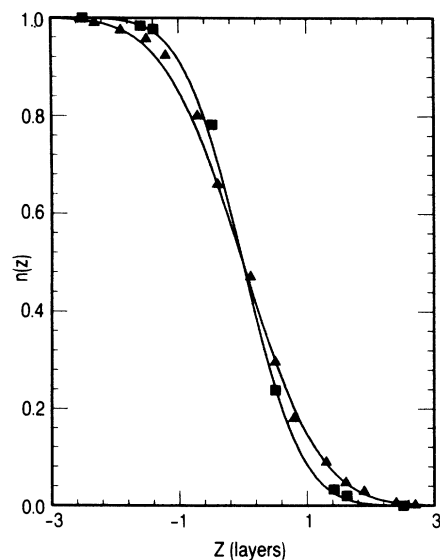


FIG. 9. For $d=3$ we plot $n(z)$ vs z for $2g/J=0.01$ (▲) and 0.1 (■) at $T=0.8J/k$ and $L=50$. The solid lines are error function profiles with $w=0.96$ and 0.73 ; these are in each instance the values inferred from the simulations.

For the smallest values of g , the width tends to saturate at the size-limited value; at the larger values, we are no longer in the appropriate small- g regime. The data at the larger values of g fit a straight line with a slope of about 0.4, rather than the expected $\frac{1}{2}$, indicated by the solid line. The interfacial profiles at $2g/J=0.01$ and 0.1 are shown in Fig. 9: the solid lines are the error function profile, Eq. (10), with $w=0.96$ and 0.73 , respectively; these are the values determined from the simulations. The fit is not as good as in other cases presented above (and below).

B. Nonequilibrium interfaces

Our studies of nonequilibrium interfaces are concerned with the interfaces between growing wetting films and the coexisting bulk phase. We have done simulations of systems with $d=2$ and 3 , but only for $d=2$ are the results unequivocal; we begin our presentation with this case. Using substrate potentials as given in Eqs. (4) and (5), with $p=1$ and 2 in the latter case, $L=1000$, $T=0.5J/k$, and starting from an initial configuration with all $h_i \equiv 0$, we have performed repeated runs of 10^5 MCS to obtain Γ (the results were reported in I), $w(t)$, and $n(z,t)$. Figure 10 shows a log-log plot of $w(t)$ versus t for the three cases of $V(h)$ given by Eq. (5) with $p=1$ and 2 and of $V(h)=0$, along with a line of slope $\frac{1}{4}$. The three cases are separated in the figure by plotting w , $2w$, and $4w$, respectively; in fact, the widths in all three cases are virtually indistinguishable. They all fit well the growth law $w \sim t^{1/4}$. The situation is distinctly analogous to that which arises in connection with the growth of Γ . Recall that in $d=2$ one is in the fluctuation-dominated growth regime² for Γ when $V(h)$ falls off faster than h^{-1} , and that $\Gamma \sim t^{1/4}$ in

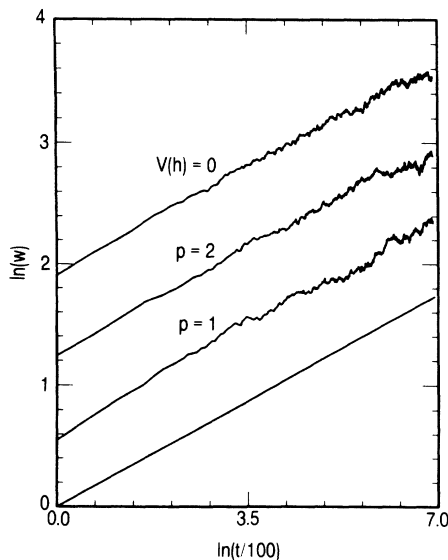


FIG. 10. In $d=2$, the logarithms of w , $2w$, and $4w$, respectively, are plotted against the logarithm of t for $V \sim h^{-p}$ with $p=1$ and 2 and for $V(h)=0$; we have used $L=1000$, and $T=0.5J/k$. A line of slope $\frac{1}{4}$ is included for comparison.

this regime; for the width, we can see from the simulation results that the substrate potential plays no role in determining $w(t)$. Even the case in the mean-field growth regime for Γ , $p=1$, shows the same behavior of w as the case of $V(h)=0$. Hence we are in all cases in the fluctuation-dominated growth regime for w . Desai and Grant¹² have used fluctuating hydrodynamics to show that the width of a liquid-vapor interface in such a situation should grow as $\sqrt{\ln t}$ in three dimensions; their argument applied to the case of two dimensions gives $w \sim t^{1/4}$ in agreement with our simulation results. Finally, we note that the simulations were done using $L=1000$, for which the size-limited width of the interface is about 12, cf. Fig. 1, the results shown in Fig. 10 are essentially in the $L \rightarrow \infty$ limit.

The profiles of the interface between the growing films and the bulk phase are shown for the case of $p=1$, at times $t=1, 10, 100, 500$, and 1000 , in units of 100 MCS, in Fig. 11. In each instance the profile is fit by an error function, Eq. (10), using the value of $w(t)$ inferred from the simulations. One can see from the figure that the profile appears to be fit quite well by this function. The conclusion that may be drawn is that the profile attains its eventual equilibrium form, if not its width, quite early during the film growth process. The profiles for the other cases treated behave in the same manner.

In three dimensions, the width of the interface is very small, the size-limited width, Fig. 6, being of order unity, and our simulations of the interface are not very informative regarding the rate at which w grows. For example, we show in Fig. 12 w^2 as a function of $\ln t$ for $L=100$, $T=0.8J/k$, and substrate potentials $V(h) \sim h^{-1}$ and $V(h)=0$. Notice that at long times the width saturates

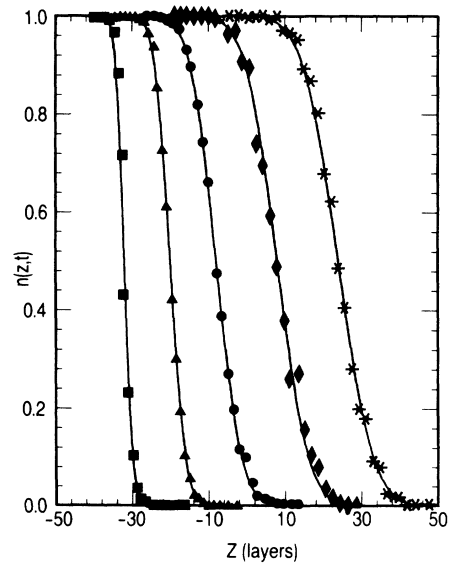


FIG. 11. For $d=2$, we plot the density $n(z,t)$ of growing wetting films against z . The substrate potential is of the form $V \sim h^{-1}$; $T=0.5J/k$, $L=400$, and $t=1$ (■), 10 (▲), 100 (●), 500 (◆), and 1000 (*), in units of 100 MCS. The solid lines show the error function profiles, Eq. (10), using values of w taken from the simulations.

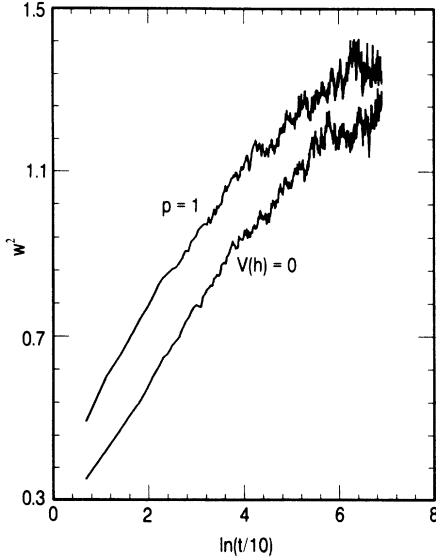


FIG. 12. In $d=3$, w^2 is plotted against $\ln t$ for growing wetting films at $L=100$ and $T=0.8J/k$ for $V \sim h^{-1}$ and $V(h)=0$.

to the size-determined value. On the basis of the simulations, we can say that $w(t)$ appears to grow no faster than some nominal power of the logarithm of t , given the potentials we have used. Also our results are at least consistent with the theoretical prediction,¹² although other interpretations are no doubt equally possible. We tentatively conclude that w grows at the appropriate rate for the fluctuation regime in three dimensions. Results found using other potentials, e.g., $V(h) \sim h^{-2}$, are no different.

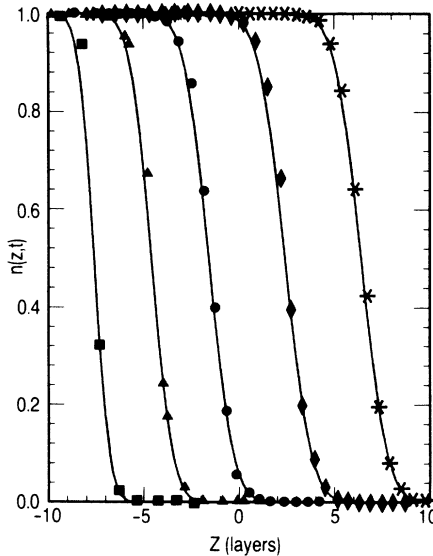


FIG. 13. For $d=3$ we plot the profiles $n(z,t)$ of growing wetting films against z . The substrate potential is of the form $V \sim h^{-1}$; $T=0.8J/k$, $L=50$, and $t=1$ (■), 10 (▲), 100 (●), 500 (◆), and 1000 (*), in units of 10 MCS. The solid lines show the error function profiles using values of w taken from the simulations.

Figure 13 shows the profiles of the growing films at times 1, 10, 100, 500, and 1000 in units of 10 MCS for $L=50$. The solid lines are the error function profile with widths of 0.64, 0.88, 1.01, 1.08, and 1.08, respectively; the width has saturated to the size-limited value at the longer times.

IV. DISCUSSION

Our simulations of equilibrium interfaces have without exception supported the predictions of exact and approximate analytic theoretical calculations of the dependence of the width on L , the system size in directions parallel to the interface, and on g , the gravitational field. In addition, we find that the profiles are in every case well-fit by error functions, Eq. (10), faces between growing wetting films and a bulk phase, we have found that the widths grow (until size effects cause saturation) with time dependences which are expected¹² in the fluctuation regime. It is interesting that this rate turns out to be the same, in the case of $d=2$, as the rate at which Γ grows in the fluctuation regime. Hence the interface between the growing film and the bulk phase is not well defined in the sense that its width is of the same order as the film thickness. Our conclusion appears to be well established by the simulations in $d=2$ and less well so in three dimensions; we can at least say in the latter instance that our results are consistent with this hypothesis.

In no case that we have considered does the presence or form of the substrate potential appear to have any effect on the rate of growth of the interfacial width, including those cases which are in the mean-field growth regime for the coverage Γ . The reason probably lies in the fact that the adsorbate-substrate energy E_V associated with having an interface of width w is of order

$$E_V \sim [w(t)/\Gamma(t)]^2 E_C, \quad (11)$$

where E_C is the interface free energy arising from capillary fluctuations. Consequently, the growth of the interface is expected to be dominated by the fluctuations and so to be independent of the actual form of V .

The profiles of the growing films are found to fit the error function form, Eq. (10), at essentially all values of the time using $w(t)$ as found from the simulations via Eq. (7). They become equilibrium, size-limited, profiles quite early in the growth process, i.e., while the film is still growing at an appreciable rate. This behavior has previously been found in the context of a time-dependent Landau-Ginzburg model.¹³

ACKNOWLEDGMENTS

The simulations described herein were performed on the Ohio State University IBM 3081, the Ohio State University of Physics VAX 8600, and the Ohio Supercomputer Center Cray X-MP. Support from National Science Foundation Grant Nos. DMR 8404961 and DMR 8705606 is gratefully acknowledged.

APPENDIX

In this appendix we reproduce as a matter of convenience, the analytic solution of the equilibrium $d=2$ model in the continuum limit with g sufficiently small but not equal to zero. The solution of this particular model was originally given by van Leeuwen and Hilhorst;³ a related model was solved by Burkhardt.⁴ We follow the exposition of the former authors and extend it to find both formal and useful results for the height-height correlation function.

Our starting point is the Hamiltonian

$$\mathcal{H} = (J/2) \sum_{i=1}^N |h_i - h_{i+1}| + \sum_{i=1}^N U(h_i). \quad (\text{A1})$$

The free energy is given by

$$F = -kT \ln \left[\sum_{\{h_i\}} \exp[-\beta\mathcal{H}(\{h_i\})] \right], \quad (\text{A2})$$

and the statistical average of any quantity $A(\{h_i\})$ is

$$\langle A \rangle = \sum_{\{h_i\}} A(\{h_u\}) \exp[\beta F - \beta\mathcal{H}(\{h_i\})]. \quad (\text{A3})$$

Define the transfer matrix as

$$M_{h,h'} = \exp[-(\beta J/2) |h - h'| - \beta U(h')]. \quad (\text{A4})$$

Now we have an eigenvalue problem,

$$\sum_{h'} M_{h,h'} \phi_h = \lambda \phi_h \quad (\text{A5})$$

such that the free energy is given by

$$F = -NkT \ln \lambda_{\max} \quad (\text{A6})$$

as $N \rightarrow \infty$. In this equation, λ_{\max} is the largest eigenvalue; let the eigenvector corresponding to this eigenvalue be ϕ_h^{\max} .

It can be shown, Eq. (1.13) of Ref. 3, that the profile is given by

$$n(z) = \langle \Theta(h_i - z) \rangle = \frac{\sum_{h \geq z} [\phi_h^{\max}]^2 e^{-\beta U(h)}}{\sum_h [\phi_h^{\max}]^2 e^{-\beta U(h)}}. \quad (\text{A7})$$

Similarly, we have found that the height-height correlation function can be written as

$$H(k) = \langle h_i h_j \rangle = (\lambda_{\max})^{-|i-j|} \times \frac{\sum_{\alpha} (\lambda_{\alpha})^{|j-i|} \left[\sum_h h e^{-\beta U(h)} \phi_h^{\alpha} \phi_h^{\max} \right]^2}{\sum_h (\phi_h^{\max})^2 e^{-\beta U(h)}}, \quad (\text{A8})$$

where λ_{α} is the α^{th} eigenvalue with corresponding eigenvector ϕ_h^{α} .

The eigenvalue problem can be converted to a discretized Schrödinger problem with the form

$$[-\Delta_2 + V(h)]\phi_h = E\phi_h, \quad (\text{A9})$$

where

$$\Delta_2 \phi_h \equiv \phi_{h-1} - 2\phi_h + \phi_{h+1}, \quad (\text{A10})$$

$$V(h) = -2\lambda^{-1} \sinh(\beta J/2) \exp[-\beta U(h)], \quad (\text{A11})$$

and

$$E = -4[\sinh(\beta J/4)]^2. \quad (\text{A12})$$

Following Ref. 3, we make the continuum limit approximation in which one replaces Δ_2 by d^2/dh^2 . For $U(h) = gh^2$ and sufficiently small g , exponential functions of $U(h)/kT$ may be expanded to first order in βg . As a consequence of these two approximations the Schrödinger equation becomes

$$\left[-\frac{d^2}{dy^2} + y^2 \right] \phi(y) = \epsilon \phi(y), \quad (\text{A13})$$

with

$$\lambda = [\coth(\beta J/4)](1 - \beta g h_0^2 \epsilon), \quad (\text{A14})$$

and

$$h = h_0 y, \quad (\text{A15})$$

where

$$h_0 \equiv [2 \sinh(\beta J/4)]^{-1/2} (\beta g)^{-1/4}. \quad (\text{A16})$$

Equation (A13) is the Schrödinger equation of a harmonic oscillator; the ground-state energy eigenvalue corresponds to the largest eigenvalue λ_{\max} . Given the well-known eigenvalues and eigenvectors of the harmonic oscillator problem, one can easily find the profile of the interface and the height-height correlation function. We find for the profile

$$n(z) = [1 - \text{erf}(z/\sqrt{2}w)]/2, \quad (\text{A17})$$

where the width w is

$$w^2 = \langle h_i h_i \rangle = h_0^2 / [2(1 + \beta g h_0^2)], \quad (\text{A18})$$

and the error function is

$$\text{erf}(x) = \frac{2}{\sqrt{\pi}} \int_0^x dt e^{-t^2}. \quad (\text{A19})$$

Further, we find that the correlation function is given by

$$\begin{aligned}
 H(k) &= w^2 f(k) \\
 &= w^2 B^{-3/2} \sum_{n=0}^{\infty} \left[\frac{1 - \beta g h_0^2}{1 - \beta g h_0^2 (4n + 3)} \right]^{-k} \\
 &\quad \times \frac{(2n + 1)!!}{(2n)!!} (1 - 1/B)^{2n},
 \end{aligned} \tag{A20}$$

where $B = 1 + \beta g h_0^2$.

In the limit of small $\beta g h_0^2 \ll 1$, we have more simply

$$\begin{aligned}
 f(k) &\approx (1 + \beta g h_0^2)^{-3/2} e^{-2\beta g h_0^2 k} \sum_{n=0}^{\infty} \frac{(2n + 1)!!}{(2n)!!} \\
 &\quad \times (\beta g h_0^2 e^{-2\beta g h_0^2 k})^{2n} \\
 &\approx e^{-2\beta g h_0^2 k} \equiv e^{-k/L_c},
 \end{aligned} \tag{A21}$$

where we have defined the correlation length $L_c \equiv (2\beta g h_0^2)^{-1} \propto g^{-1/2}$. Our result for the correlation function predicts that a plot of $\ln[f(k)]/\beta g h_0^2$ versus k should be a straight line, independent of g , with a slope of -2 .

¹Z. Jiang and C. Ebner, Phys. Rev. B **36**, 6976 (1987).

²R. Lipowsky, J. Phys. A **18**, L585 (1985).

³J. M. J. van Leeuwen and H. J. Hilhorst, Physica **107A**, 319 (1981).

⁴T. Burkhardt, J. Phys. A **14**, L63 (1981).

⁵A. Ciach, Phys. Rev. B **34**, 1932 (1986).

⁶A. Ciach and J. Stecki, J. Phys. A **20**, 5619 (1987).

⁷D. Bedeaux, J. D. Weeks, and B. J. A. Zielinska, Physica **130A**, 88 (1985).

⁸D. B. Abraham and P. Reed, Phys. Rev. Lett. **33**, 377 (1974).

⁹D. B. Abraham, Commun. Math. Phys. **49**, 35 (1976).

¹⁰F. P. Buff, R. A. Lovett, and F. H. Stillinger, Phys. Rev. Lett. **15**, 621 (1965).

¹¹D. Bedeaux and J. D. Weeks, J. Chem. Phys. **82**, 972 (1985).

¹²R. C. Desai and M. Grant, in *Fluid Interfacial Phenomena*, edited by C. A. Croxton (Wiley, New York, 1986), p. 135.

¹³I. Schmidt and K. Binder, Z. Phys. B **67**, 369 (1987).

¹⁴J. D. Weeks, in *Ordering in Strongly Fluctuating Condensed Matter Systems*, edited by T. Riste (Plenum, New York, 1980), p. 293.